Feasibility of Using the O-Arm Imaging System During ENB-rEBUS–guided Peripheral Lung Biopsy

A Dual-center Experience

Roy J. Cho, MD, Michal Senitko, MD,† Jennifer Wong, MD,**
Erhan H. Dincer, MD, Hamid Khosravi, PhD,‡*
and George E. Abraham III, MD§

Background: **There is a paucity of real-time imaging modalities available for the bronchoscopic biopsy of peripheral lung nodules. We aim to demonstrate the feasibility of the O-arm imaging system to guide real-time biopsies of peripheral lung nodules during electromagnetic navigation bronchoscopy.**

Methods: **A retrospective review was performed at 2 academic medical centers utilizing O-arm guidance.**

Results: **The average nodule size was 2.1×2.0 cm and were mostly solid (66%) with a positive bronchus sign (83%). O-arm imaging confirmed tool-in-lesion in all cases. The diagnostic yield was 33%. Four cases were nondiagnostic of the 6 cases performed. In these cases, necrotic tissue was the most common (75%) and showed resolution following subsequent imaging. The average 3-dimensional (3D) spin time was 23.5 seconds. The average number of 3D spins performed per case was 4.33. The average effective dose per 3D spin was 3.73 mSv.**

Conclusion: **We have demonstrated the O-arm's feasibility with electromagnetic navigation bronchoscopy for peripheral lung nodules. The O-arm was able to confirm tool-in-lesion in all cases which added confidence to the biopsy. Four high-resolution 3D spins per case may limit the total computed tomography effective dose. We also noted that both metal and radiation scatter were minimal when appropriate radiation safety standards were met. Although additional experience and data will be required to verify the O-arm approach for routine use, our initial experience is promising.**

Key Words: navigational bronchoscopy, peripheral lung nodules, lung cancer, O-arm

(*J Bronchol Intervent Pulmonol* 2020;00:000–000)

The estimated frequency of lung nodules is ~40% to 60% in lung cancer screening trials using low-dose computed tomography (CT) and a further increase is expected as lung cancer screening becomes more commonplace.[1–5] The Fleischner Society has developed guidelines to risk stratify nodules and includes an algorithm to either continue imaging surveillance, pursue advanced imaging (ie, positron emission tomography-CT), or perform tissue sampling.[6] The current approach for tissue sampling includes surgical resection, transthoracic needle aspiration biopsy with CT or ultrasound, or bronchoscopy. The latter has gained attention given its low risk for postbiopsy pneumothorax, minimally invasive approach, and ability to perform mediastinal staging in the same setting.[7] In addition, rapidly developing technology in this space has increased the fidelity of the procedure among pulmonologists as these are now guided by electromagnetic navigation bronchoscopy (ENB), radial endobronchial ultrasound (rEBUS), robotic assistance, and augmented imaging (multiplane fluoroscopy and cone-beam volume CT). A cone-beam CT image reconstruction widely used by other procedural specialties provides real-time imaging confirmation of tool-in-lesion and is associated with higher navigation confidence and diagnostic yield during ENB-rEBUS–guided biopsies.[8] Another real-time imaging device, O-arm O2 Imaging System (Medtronic, Minneapolis, MN), is an intraoperative 2-dimensional (2D)/3D imaging system mostly used during orthopedic and neurosurgical operations because of its ability to highlight anatomic structures and objects with high x-ray attenuation such as bony anatomy and metallic objects. One study has demonstrated its use for intraoperative localization of

Received for publication July 1, 2020; accepted November 10, 2020.
From the *Department of Pulmonary, Allergy, Critical Care and Sleep Medicine, University of Minnesota, Minneapolis, MN; Departments of †Medicine and Surgery; ‡Radiology; and §Medicine, University of Mississippi Medical Center, Jackson, MS.
R.J.C. and M.S. contributed equally.
Disclosure: There is no conflict of interest or other disclosures.
Reprints: Roy J. Cho, MD, Department of Pulmonary, Allergy, Critical Care and Sleep Medicine, University of Minnesota, 401 East River Parkway Suite 350, MMC 276; Room VCRC 450, Minneapolis, MN 55455 (e-mail: choxx548@umn.edu).

DOI: 10.1097/LBR.0000000000000738

nodules for patients undergoing video-assisted thoracoscopic surgery; however, its potential use with ENB to provide real-time confirmation of navigation success and tool-in-lesion has not been previously described.[9] We present a retrospective review of cases testing the feasibility of O-arm imaging during ENB-guided biopsy of peripheral lung nodules among 2 academic centers.

METHODS

We have reported all cases (n = 6) between 2 academic medical centers in the United States testing the O-arm Imaging System with ENB-rEBUS–guided bronchoscopy. This did not meet the federal definition of human research; therefore, was not subject to IRB review.

A single-interventional pulmonologist at each center performed all center-reported procedures under general anesthesia in an operating/procedure room, which met radiation safety criteria. Lesion location, peripherality, size, and presence of a bronchus sign was determined from diagnostic CT or positron emission tomography-CT scans. All cases were done under general anesthesia utilizing center-specific anesthesia protocols for ventilation, oxygenation, and utilization of neuromuscular agents. Anesthesia time (minutes) was defined as time from initial anesthetic administration to recovery room entrance. Procedural time (minutes) was defined as the beginning of the time-out protocol and the end of the postprocedure debriefing. In both centers, the mediastinal staging was established before nodule biopsy with a convex EBUS bronchoscope (Olympus) and peripheral nodule biopsy was accomplished using BF-1T180 flexible bronchoscope (Olympus), Super Dimension v7.2 (Medtronic), and 20 mHz radial ultrasound probe (Olympus). ENB-rEBUS were conducted per established protocols. Utilization of rapid on-site cytology was at the discretion of the operator.

After validating navigation success with ENB-rEBUS, the bronchoscope was secured in place using a transesophageal transducer holder (Civco Medical Solutions, Coralville, IA). The O-arm was then positioned over the patient's mid-to-upper chest and the target field was verified with a low-definition 3D scan, confirming visibility of the lesion. Before the 3D spin, all staff left the room and stood behind a radiation safety-approved door. The number of 3D spin reconstructions performed was at the discretion of the operator. Both centers performed all of the 3D spin reconstructions under high-resolution protocol. Once tool-in-lesion was confirmed, subsequent biopsies were performed. Tool utilization and number of repeat 3D spins were performed at the discretion of the operator, and the utilization of a pulsed 2D fluoroscopy mode. Diagnostic yield was defined as those that yielded a malignant or specific benign diagnosis.[10] The endpoint for this feasibility study was successful identification of the lesion, tool, and/or tool-in-lesion with the O-arm device.

RESULTS

Patient characteristics and information regarding nodule specifics and biopsy results are demonstrated in Table 1. A total of 6 ENB-rEBUS cases were performed (cases 1 to 3 and 4 to 6 from the University of Mississippi and Minnesota; respectively) utilizing O-arm imaging. The target nodule had an average size of 2.1×2.0 cm and were mostly solid (66%) with a positive bronchus sign in 83% of the cases. We identified a concentric pattern in 2 cases (33%) and an eccentric pattern in 4 cases (67%) with rEBUS of the target lesion (Table 2). The diagnostic yield was 33% (2 cases: adenocarcinoma and necrotizing granuloma). Four were nondiagnostic of the 6 cases performed. In these cases, necrotic tissue was the most common (75%).

All targets were located in either the right lower lobe (50%) or left upper lobe (50%). Only 1 case demonstrated atelectasis with O-arm. There were no complications related to the biopsy and all patients were discharged home following the procedure. O-arm imaging confirmed good visibility of the margins of a targeted lesion and tool-in-lesion in all the cases (Table 2; Fig. 1). There was no difference in the visibility of different tools and their position with respect to the targeted lesions with O-arm (Figs. 2, 3).

The summary of radiation exposure per case is illustrated in Table 3. The average 3D spin time was 23.5 seconds. The average number of 3D spins per case was 4.33 with an average effective dose of 3.73 mSv per spin. Longer times of a pulsed 2D fluoroscopy mode on the O-arm for cases 5 and 6 led to fluoroscopy-effective doses ranging between 8.7 and 11.2 mSv.

DISCUSSION

The O-arm platform is designed to highlight bone density specifically for orthopedic and neurosurgical operations. In our institutions, we do not have a cone-beam CT integrated into our procedural suite; therefore, we used the O-arm to offer similar real-time confirmation of tool-in-lesion, which has not been previously described in the literature. Although portable, the O-arm has a significant footprint of 110.5×32×79.6"

TABLE 1. Patient Characteristics

	Age	Sex	Tobacco (Pack-Year, Status)	Lesion Location, Peripherality, Size, and Morphology	pCA	Lesion SUV (g/mL)	Procedure Indication	Biopsy Results	Follow-up
Case 1	72	Female	Never smoker	RLL, outer, 2.6×1.7 cm, solid	NA	4.1	Previous malignancy, growing nodules	Nondiagnostic	Contralateral endobronchial lesion with metastatic salivary gland carcinoma
Case 2	63	Male	40, current smoker	LUL, outer, 1.9×1.4 cm, solid	High	5.8	Growing nodule	Inflammatory and necrotic cells, BAL grew Penicillium species	Improved on follow-up imaging
Case 3	70	Male	30, former smoker	RLL, outer, 2.9×1.7 cm, cavitary	High	3.7	Growing nodule	Adenocarcinoma, pathologic stage IB	RLL lobectomy
Case 4	67	Male	> 50, current smoker	LUL, outer, 1/3, 2.4×3.4 cm, cavitary	High	4.5	Growing nodule	Necrotizing granuloma, negative cultures	Improved on follow-up imaging
Case 5	70	Male	40, current smoker	LUL, outer, 1/3, 1.8×1.6 cm, solid	High	6	Growing nodule	Inflammatory and necrotic cells, negative cultures	Improved on follow-up imaging
Case 6	55	Male	48, current smoker	RLL, outer, 1/3, 1.8×1.5 cm, solid	High	5.2	Growing nodule	Inflammatory and necrotic cells, negative cultures	Improved on follow-up imaging

BAL indicates bronchoalveolar lavage; LUL, left upper lobe; pCA, pretest probability of lung cancer; RLL indicates right lower lobe; SUV, standardized uptake value of positron emission tomography.

TABLE 2. Procedural and Lesion Characteristics by Imaging Modality

	Anesthesia (min)	Procedure (min)	EBUS Mediastinal Staging	CT Bronchus Sign	rEBUS Pattern	O-Arm Confirmation	Tools Used
Case 1	140	120	3 mediastinal LN sampled before peripheral biopsies	Yes	Eccentric	Lesion+TIL	rEBUS, 21G needle
Case 2	137	100	3 mediastinal LN sampled before peripheral biopsies	Yes	Concentric	Lesion+TIL	rEBUS, 21G needle, triple needle brush, forceps
Case 3	114	95	3 mediastinal LN sampled before peripheral biopsies	Yes	Eccentric	Lesion+TIL	rEBUS, 21G needle, triple needle brush, forceps
Case 4	70	50	4 mediastinal LN sampled before peripheral biopsies	Yes	Concentric	Lesion+TIL	rEBUS, 21G needle, triple needle brush, forceps
Case 5	80	60	3 mediastinal LN sampled before peripheral biopsies	Yes	Eccentric	Lesion+TIL	rEBUS, triple needle brush
Case 6	92	72	3 mediastinal LN sampled before peripheral biopsies	No	Eccentric	Lesion+TIL	rEBUS, triple needle brush

CT indicates computed chest tomography; G, gauge; LN, lymph node; rEBUS, radial endobronchial ultrasound probe; TIL, tool-in-lesion.

FIGURE 1. Computed tomography (CT) and associated O-arm images. Image demonstrates a left upper lobe nodule on CT (left) and O-arm–guided electromagnetic navigation bronchoscopy + radial endobronchial ultrasound (rEBUS) where the tip of the rEBUS probe is demonstrated (right).

(280.6×81.3×202.2 cm) with a weight of 925.8 kg. Its gantry opening is 27.5" (69.9 cm) with a bore diameter of 38" (96.5 cm) (Fig. 4A). The device with an open gantry (appearance of letter C) slides over a standard fluoroscopy bed and it is easily maneuvered to the desired position. Once positioned the gantry is closed which provides a letter O appearance and the device is ready to be used. The settings can be adjusted on a system panel as described in Figure 4B. The O-arm platform can provide multiple imaging modalities including single-plane 2D, multiplane 2D, standard 3D volumetric, high-definition 3D volumetric, low-dose 3D volumetric, and enhanced cranial 3D volumetric. The single-plane 2D is pulsed fluoroscopy at 30 frames/second, whereas multiplane 2D can provide up to 4

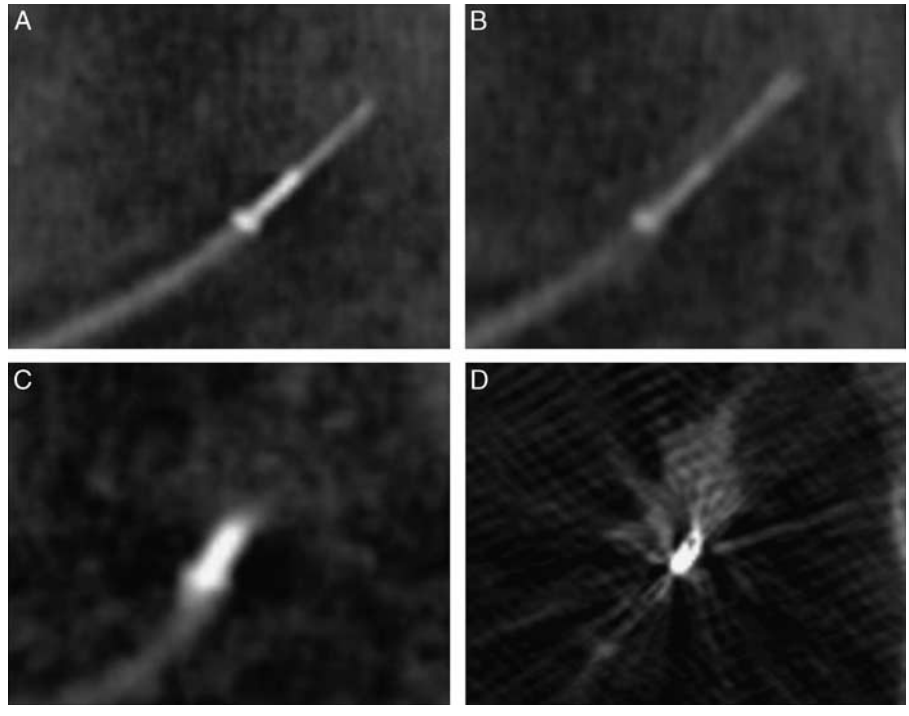

FIGURE 2. O-arm images of different tools within a lesion. A, FNA needle; triple needle brush (B); tip ofradial EBUS probe (C); and biopsy forceps (D). FNA indicates fine needle aspiration.

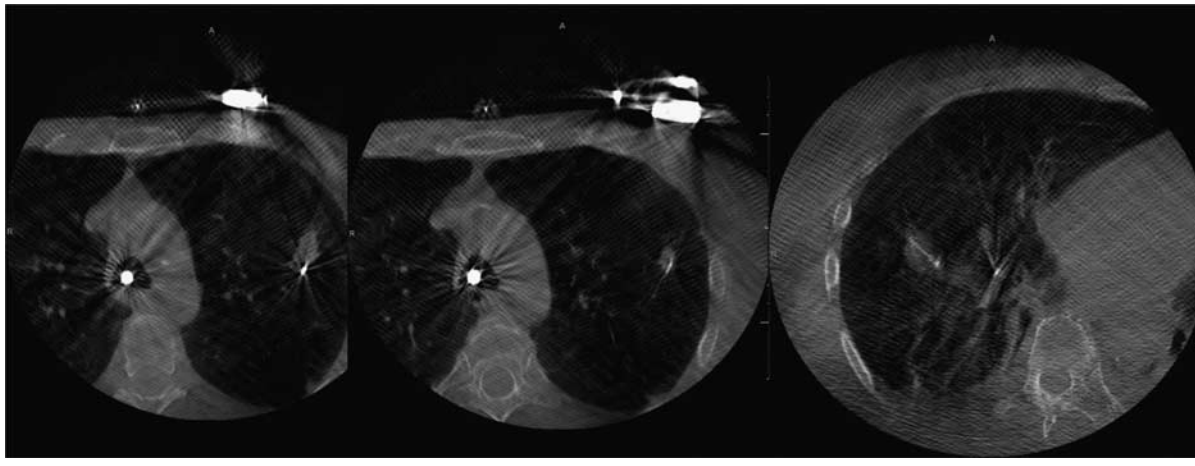

FIGURE 3. O-arm images of tool-in-lesion. Forceps (left), triple needle brush (middle), and FNA needle (right). FNA indicates fine needle aspiration.

2D images from pre-set positions. The high-definition 3D volumetric mode provides a standard of 27 seconds for data acquisition and 23 seconds for 3D reconstruction with 754 images over 360 degrees with a resolution (mm) of 0.415×0.415×0.833 (20 cm field of view) or 0.775×0.775×0.833 (40 cm field of view). The manufacture reported effective dose (mSv) for the chest region is 2.99 (high definition) and 1.88 (low definition) versus 3.46 for a standard chest CT. In this study, the calculated average effective dose was 3.73 mSv. This suggests the O-arm doses are comparable with CT. The images are reconstructed and displayed on a portable screen with an ability to scroll through 3 different planes with a mouse control.

In this feasibility study, we demonstrated that the O-arm was able to assist ENB-rEBUS during peripheral lung nodule biopsies. The lung parenchyma was well visualized as was the target nodule. The O-arm was able to demonstrate tool-in-lesion which added to the confidence of the biopsy in all 6 cases. Unlike 2D projection fluoroscopy, the 2D axial views provided by O-arm allowed us to identify the biopsy tool and confirm its position in relation to the target (Figs. 1–3). This was specifically highlighted in case 3 where the O-arm disproved the ENB target lesion location which led to repeating the electromagnetic navigation part of the procedure. However, in the subset of patients (cases 1 to 3) where the position of each tool was confirmed with a high-definition 3D spin, the total effective dose was much higher than a standard chest CT or cone-beam CT (Table 3), which has been reported to be between 7.6 and 15.1 mSv with lower and upper thoracic biopsies.[8] In this study, the average effective dose in high-definition mode was 3.73 mSv per 3D spin. The total effective dose was > 20 mSv when more than 5 spins were performed or with longer pulsed 2D fluoroscopy time. The effective fluoroscopy dose is directly proportional to exposure times which seemed to be higher for cases 5 and 6 with higher fluoroscopy times (few minutes) in comparison with other cases fluoroscopy time in about a couple of seconds. This was because of more biopsy tools and passes performed for cases 4 to 6. Therefore, performing less than 4 3D spins per case, utilizing a low-dose mode and a reasonable use of 2D-pulsed fluoroscopy could potentially lead to a dose comparable with CT-guided procedures (< 15 mSv). More data will be needed to confirm this observation.

As the O-arm typically reconstructs the images on the basis of bone windows; metal scatter prohibiting an identifiable lung image was a concern. Therefore, we performed a dry-run procedure in the operating room suite before the first case to determine the degree of metal scatter. An airway mannequin (TruCorp, North Ireland) previously registered with

TABLE 3. Effective Doses With O-Arm Guidance

	3D Spin Time (s)	No. 3D Spins	CT Effective Dose (mSv)	FL Time (s)	FL Effective Dose (mSV)	Total FL+ CT (mSV)
Case 1	23	5	22.90	0.53	0.01	22.91
Case 2	24	5	22.55	0.1	0.13	22.68
Case 3	24	9	35.15	0.81	0.05	35.2
Case 4	23	1	3.66	2.73	0.09	3.75
Case 5	24	3	8.79	226.73	11.22	20.01
Case 6	23	3	8.55	206.34	8.79	17.34

3D indicates 3-dimensional; CT, computed tomography; FL, fluoroscopy.

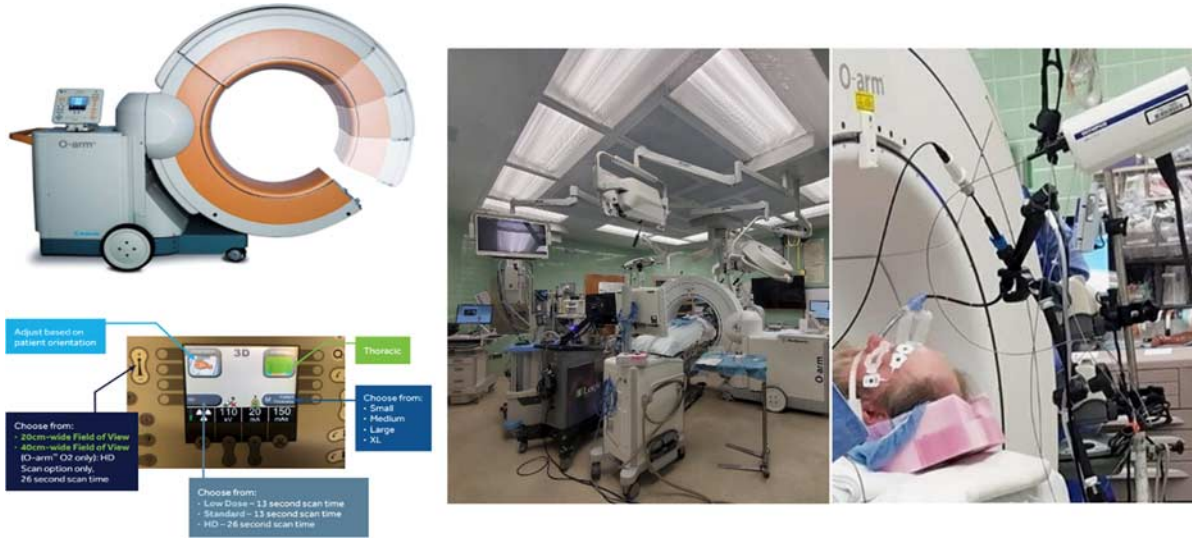

FIGURE 4. Left, The O-arm platform with a gantry opening and detail of the system panel with the description of the setting options. Right, Intraoperative layout and close view of scope holder.

the Super Dimension software was used for the test. The O-arm was positioned over the mannequin on the Super Dimension bed and both low-definition and high-definition scans were performed. In this exercise, the degree of metal scatter was minimal from supportive devices, navigation hardware, and bronchoscope. We were impressed by the lack of metal scatter and high-quality images of both the lung parenchyma and the target nodule. Though not able to clearly see small airways, this did not affect our ability to localize a tool within a lesion.

Surgical staff will be exposed to scattered radiation during O-arm 2D fluoroscopy and/or 3D acquisitions; therefore, procedural rooms have to meet appropriate radiation safety standards during use. The surgical staff may reduce their exposure by moving to predetermined locations while remaining in the operating/procedure room during acquisition. Standing beyond a 2-m distance from the isocenter during a single 3D image acquisition would expose the staff to <10 μSv. The lowest exposure location is behind the control panel, where the O-arm operator is typically positioned, as the O-arm gantry and provided shield attenuate x-rays produced during imaging.[11] Assuming 100 cases per year with an average of 4.3 spins per patient workload, an unprotected staff would be expected to receive below 5 mSv a year at a distance of 2 m from the patient's chest. The occupational exposure limit is 50 mSv per year in the United States and individual dosimetry readings are used to monitor employees' exposure. That being said, surgical staff members may stay inside the operating room during O-arm 3D acquisition, but it is still recommended they stay as far away as possible from the isocenter, wear personal protective equipment such as lead aprons, goggles and thyroid shields, or position themselves behind lead screens.

A logistical issue to consider before using the O-arm for ENB is its significant footprint (Fig. 4). The size of the O-arm requires a larger room and additional time is added to the procedure for appropriate positioning and calibration. Because of the portability its use is not limited to a dedicated room. As always, workflow obstructions were mitigated by preprocedure planning.

We have demonstrated the feasibility and technical aspects of O-arm guidance with ENB-rEBUS. We have demonstrated that a target lesion within lung parenchyma can be clearly seen with the ability to verify tool-in-lesion. We demonstrated that performing less than 4 high-resolution 3D spins per case can limit the CT effective dose. We also note that metal scatter and radiation scatters are minimal when appropriate radiation safety standards are met. Overall, we were impressed with the high-quality lung images acquired with the O-arm which has not previously been demonstrated in the literature. The anesthesia and procedure time were longer in the cases with a higher number of 3D scans. To our knowledge, this is the first description of O-arm guidance for ENB tool-in-lesion confirmation. Future studies are needed to define the optimal imaging parameters, technique, and overall relevance to histologic yield.

CONCLUSIONS

We demonstrated that the O-arm can be used to confirm ENB localization of a peripheral nodule and can verify tool-in-lesion. Although more experience and data will be required to verify the O-arm approach, our initial experience is promising.

REFERENCES

1. Ost D, Fein AM, Feinsilver SH. Clinical practice: the solitary pulmonary nodule. *N Engl J Med*. 2003;348:2535–2542.
2. Diederich S, Wormanns D, Semik M, et al. Screening for early lung cancer with low-dose spiral CT: prevalence in 817 asymptomatic smokers. *Radiology*. 2002;222:773–781.
3. McWilliams A, Mayo J, MacDonald S, et al. Lung cancer screening: a different paradigm. *Am J Respir Crit Care Med*. 2003;168:1167–1173.
4. Swensen SJ, Jett JR, Hartman TE, et al. CT screening for lung cancer: five-year prospective experience. *Radiology*. 2005;235:259–265.
5. van Klaveren RJ, Oudkerk M, Prokop M, et al. Management of lung nodules detected by volume CT scanning. *N Engl J Med*. 2009;361:2221–2229.
6. MacMahon H, Austin JH, Gamsu G, et al. Guidelines for management of small pulmonary nodules detected on CT scans: a statement from the Fleischner Society. *Radiology*. 2005;237:395–400.
7. Cox JE, Chiles C, McManus CM, et al. Transthoracic needle aspiration biopsy: variables that affect risk of pneumothorax. *Radiology*. 1999;212:165–168.
8. Pritchett MA, Schampaert S, de Groot JAH, et al. Cone-beam CT with augmented fluoroscopy combined with electromagnetic navigation bronchoscopy for biopsy of pulmonary nodules. *J Bronchol Intervent Pulmonol*. 2018;25:274–282.
9. Ohtaka K, Takahashi Y, Kaga K, et al. Video-assisted thoracoscopic surgery using mobile computed tomography: new method for locating of small lung nodules. *J Cardiothorac Surg*. 2014;20:1–7.
10. Silvestri GA, Bevill BT, Huang J, et al. An evaluation of diagnostic yield from bronchoscopy: the impact of clinical/radiographic factors, procedure type, and degree of suspicion for cancer. *Chest*. 2020;157:1656–1664.
11. Pitteloud N, Gamulin A, Barea C, et al. Radiation exposure using the O-arm surgical imaging system. *Eur Spine J*. 2017;26:651–657.